Available online at www.sciencedirect.com
SCIENCE DIRECT
Thermochimica Acta 443 (2006) 183–188
thermochimica acta
www.elsevier.com/locate/tca

Kinetic parameters of surfactant remotion occluded in the pores of the AlMCM-41 nanostructured materials

Marcelo J.B. Souza [a], Antonio S. Araujo [b,*], Anne M.G. Pedrosa [b], Stevie H. Lima [b], Valter J. Fernande Jr. [b]

[a] *Department of Chemical Engineering, Federal University of Sergipe, 49100-000 São Cristovão, Sergipe, Brazil*
[b] *Department of Chemistry, Federal University of Rio Grande do Norte, CP1662, 59078-970 Natal, RN, Brazil*

Received 19 September 2005; received in revised form 20 December 2005; accepted 24 December 2005
Available online 21 February 2006

Abstract

A series of AlMCM-41 molecular sieves was synthesized starting from a hydrogel with the following molar composition: 1CTMABr: $4.58SiO_2$:$(0.437 + X)Na_2O$:XAl_2O_3:$200H_2O$. Tetramethylammonium silicate (TMAS) was used as silicon source and cethyltrimethylammonium bromide (CTMABr) was used as structure template. The obtained materials were characterized by nitrogen adsorption, XRD, FT-IR and TG/DTG. Model-free kinetic algorithms were applied in order to determinate conversion, isoconversion and apparent activation energy to decomposition of CTMA+ species from the AlMCM-41 materials with different silicon/aluminium (Si/Al) ratios of 20, 40, 60 and 80.
© 2006 Elsevier B.V. All rights reserved.

Keywords: AlMCM-41; Si/Al ratio; CTMA+; Model-free kinetics

1. Introduction

Silica-based M41S materials discovered by Mobil Company in the early 90s [1,2] are very interesting class of mesoporous materials. MCM-41 (p6*m*m) silica whose pore structure consists of hexagonally packed cylindrical is the main component of the M41S family. Hexagonal mesoporous systems with high surface area open possibilities of generate the surface acidity necessary to catalyze organic reactions as transesterification of vegetable oils producing biodiesel [3,4]. The formation of the AlMCM-41 phase occurs according to the liquid crystal template (LCT) mechanism, in which tetrahedral SiO_4 and AlO_4 species react with the surfactant template under hydrothermal conditions [5]. A typical preparation of AlMCM-41 needs basically of a solvent, a template (surfactant molecule), a silica source and an aluminium source [6–8]. In order to be used as adsorbents and catalytic applications the MCM-41 materials need to pass for a process for removal of the template molecules in the pores. Some works were published studying the removal of those template molecules, of which they are more mentioned: extraction by solvents, extraction with CO_2 and calcination [9–11]. In most of the cases authors give significant importance to the calcination for showing more efficiency and to guarantee the complete removal of CTMA+ and AlMCM-41 materials with several silicon/aluminium atomic ratios (Si/Al). The variables in a typical calcination process are time, temperature, heating rate, catalyst mass and dynamic atmosphere. In this work, thermogravimetry is used for studying the kinetic parameters of CTMA+ removal employing integral TG curves and a model-free kinetic method [12–14] to calculate the activation energy, the conversion rates and the isoconversion parameters to evaluate the stage of decomposition of removal template species as function of temperature and time under dynamic flow conditions.

2. Experimental

The AlMCM-41 materials were synthesized starting from tetramethylammonium silicate solution (TMAS, Sigma–Aldrich, $P_A = 17.5\%$) as silicon source, sodium hydroxide (VETEC, $P_B = 99\%$) as sodium source, pseudobohemite (Vista, $P_C = 70\%$) as aluminium source, cethyltrimethylammonium bromide (CTMABr, VETEC, $P_D = 98\%$) as structural template and distilled water as solvent. For the pH adjustment, 30% acetic

* Corresponding author. Tel.: +55 84 2119240; fax: +55 84 2119240.
E-mail address: asa-ufrn@usa.net (A.S. Araujo).

0040-6031/$ – see front matter © 2006 Elsevier B.V. All rights reserved.
doi:10.1016/j.tca.2005.12.022

Table 1
Molar compositions of the synthesis gels and its respective amounts in grams of the pure starting materials

Si/Al	Gel molar composition	A	B	C	D	E[a]
20	$4.58SiO_2$:$0.550Na_2O$:$0.1140\ Al_2O_3$:1CTMABr:$200H_2O$	1.747	1.159	0.042	1.318	13.019
40	$4.58SiO_2$:$0.494Na_2O$:$0.0570\ Al_2O_3$:1CTMABr:$200H_2O$	1.751	0.143	0.021	1.321	13.049
60	$4.58SiO_2$:$0.475Na_2O$:$0.0380\ Al_2O_3$:1CTMABr:$200H_2O$	1.752	0.138	0.014	1.322	13.058
80	$4.58SiO_2$:$0.465Na_2O$:$0.0285\ Al_2O_3$:1CTMABr:$200H_2O$	1.753	0.135	0.010	1.323	13.063

[a] The final value of E can be approximated by: $E_{final} = E - A((1 - P_A)/P_A))$.

acid in ethanol solution was used. Table 1 shows the hydrogel formulas and the respective mass values of the pure precursors: A (TMAS), B (NaOH), C (pseudobohemite), D (CTMABr) and E (water). The P_i value represents the purity to each precursor and it should be used to correct the values of the pure precursors showed in Table 1 to obtain the final amount of starting materials.

In a typical synthesis the chemicals were mixed in order to obtain a gel with the following molar composition: $4.58SiO_2$:$(0.437 + X)Na_2O$:1CTMABr:XAl_2O_3:$200H_2O$. The value of X represents the molar coefficient to the aluminium source. The value of X varied of 0.114, 0.0570, 0.0380 and 0.0285 in order to obtain materials with silicon/aluminium atomic ratios of 20, 40, 60 and 80, respectively. The procedure used to obtain ca. 1 g of calcined AlMCM-41 with different silicon/aluminium compositions was: (i) (A/P_A) grams of TMAS, (B/P_B) grams of NaOH, (C/P_C) grams of pseudobohemite and ($E/2$) grams of water were placed into a 100 mL Teflon Becker and stirred at 333 K for 2 h in order to obtain a clear solution; (ii) a solution prepared from (D/P_D) grams of cethyltrimethylammonim bromide and ($E/2$) grams of distilled water was added to the mixture; (iii) aged for 30 min at room temperature. The hydrogels were placed into 45 mL teflon-lined autoclaves and heated at 373 K for 3 days. Their pH was measured each day and adjusted to 9–10. In the last day was added sodium acetate (Carlo Erba) in a 1:3 M proportion of CH_3COONa/CTMABr in order to stabilize the silica [9]. The obtained materials were filtered, washed and dried at 373 K in a stove for 2 h.

XRD measurements were carried out in Shimadzu equipment using Cu Kα radiation in 2θ angle of 1–10° with step of 0.01°. FT-IR spectra were obtained in a BOMEM equipment model MB100. Surface area, pore volume and pore distribution were obtained by BET and BJH methods stating of nitrogen adsorption isotherms at 77 K (ANOVA 2000). TG analysis was carried out in Mettler equipment, TGA/SDTA851 model, using nitrogen as a gas carrier flowing at 25 mL min^{-1}. The samples as synthesized were heated at room temperature up to 1173 K, at a heating rate of 5, 10 and 20 K min^{-1}. Table 2 shows the values of the temperature removal of the CTMA+ as a function of the conversion and time. For example, to remove 95% of the template species of the AlMCM-41 with Si/Al = 40 in 60 min, temperature of 695 K is necessary and with the same time to remove 99%, 732 K is necessary. The Vyazovkin [12–14] model-free kinetics was used to evaluate the kinetic parameters of surfactant decomposition from AlMCM-41 material.

Table 2
Isoconversion parameters to removal of CTMA+ from AlMCM-41 materials (temperature in K)

Time (min)	α (%)						
	10	30	50	70	90	95	99
AlMCM-41 (Si/Al = 20)							
10	422	467	493	517	611	717	763
20	408	457	484	507	581	710	755
30	400	451	478	501	565	705	750
40	395	447	475	497	554	702	747
50	390	444	472	494	545	700	744
60	387	442	469	491	539	698	742
AlMCM-41 (Si/Al = 40)							
10	441	473	496	519	615	723	765
20	435	465	488	511	583	712	752
30	431	460	483	506	568	706	745
40	429	457	480	502	562	701	740
50	427	455	477	499	555	698	736
60	426	453	475	497	545	695	733
AlMCM-41 (Si/Al = 60)							
10	452	482	501	521	660	738	773
20	447	476	494	512	651	728	762
30	444	473	490	507	646	722	755
40	442	471	487	504	642	718	751
50	440	469	485	501	639	715	747
60	439	468	483	499	637	712	745
AlMCM-41 (Si/Al = 80)							
10	444	470	489	508	552	696	743
20	438	463	480	499	538	684	730
30	434	458	475	493	530	678	722
40	431	455	472	490	525	673	717
50	429	453	469	487	521	669	713
60	428	451	467	485	517	667	710

3. Results and discussion

The final samples of AlMCM-41 with different Si/Al ratios were obtained by calcination of the as-synthesized samples heating the materials from ambient temperature to 723 K at 10 K min^{-1} in dynamic flow of N_2 of 25 mL min^{-1} and then stayed at 723 K by 120 min. Fig. 1 shows the XRD powder patterns of the calcined AlMCM-41 samples with different silicon/aluminium ratios.

From XRD results it can be observed that the intensity of the peaks diffraction significantly decreased with increasing of Si/Al ratio except for the sample with Si/Al ratio of 40. The variation in the XRD intensities is attributed to obtaining of samples with different crystallinity degrees, which is a known behavior related to the increase of contrast between the silica–alumina

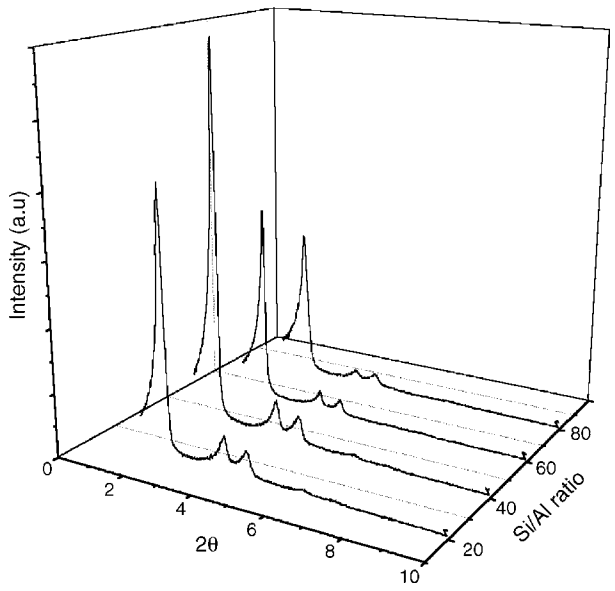

Fig. 1. XRD powder diffraction patterns of AlMCM-41 with different silicon/aluminium ratios.

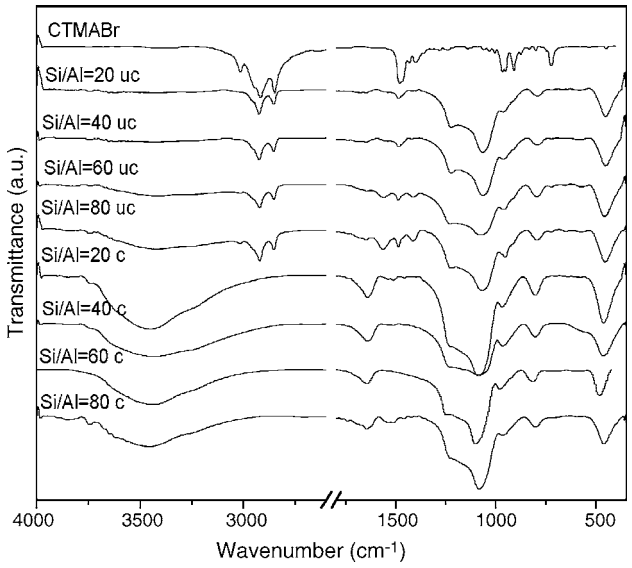

Fig. 2. FT-IR spectra of AlMCM-41 materials with different silicon/aluminium ratios, where (c) is the calcined and (uc) is the uncalcined.

wall and the pore space after the surfactant has been removed [15]. Papers show that the incorporation of aluminium in MCM-41 materials results higher degrees of crystallinity than pure siliceous MCM-41 due to obtaining of materials with larger structure stability [16,17]. All the materials showed characteristic peaks in the 2θ ranges of 1–10°, related to (1 0 0), (1 1 0), (2 1 0) Miller index, characteristics of AlMCM-41 materials [1,2]. The specific surface area was determined according to the standard Brunauer–Emmett–Teller (BET) method [18] and pore size distributions by Barrett–Joyner–Halenda (BJH) algorithm [19]. The adsorption parameters can be visualized in Table 3. In this table it can be observed that obtained materials were with significant values of superficial area, pore volume and silica–alumina wall thickness, and these properties showed dependence with the crystallinity degree showed in Fig. 1. Samples with high crystallinity degree present the highest degree of hexagonal ordination and consequently high values of specific surface area, pore diameters and pore volumes.

FT-IR analyses were useful to provide information about the efficiency of the calcination process where occurs the elimination of the CTMA+ groups from AlMCM-41 materials [20]. Fig. 2 shows the FT-IR analysis of the AlMCM-41 materials before and after the calcination. It can be observed that the CTMA+ was fully removed in the samples obtained. This can be verified by the absence of the functional groups of the CTMA+ species after a heat treatment under dynamic flow conditions. Table 4 shows the FT-IR data and its respective attributions.

In several processes, the determination of a specific chemical reaction rate depends on conversion (α), temperature (T) and time (t). The reaction rate represented as a function of conversion $f(\alpha)$ is different for each process and must be determined experimentally. For simple reactions, the evaluation of $f(\alpha)$ with the nth order is possible. For complex reactions the function of (α) is complicated and generally unknown; in these cases the nth order algorithm causes unreasonable kinetic data. With the model-free kinetics more accurate evaluations of complex reactions can be performed, as a trustworthy way of obtaining reliable and consistent kinetic information about the overall process [12]. Vyazovkin [13,14] developed an integral kinetic method where no model has to be selected (model free-kinetics) which allows to evaluate both simple and complex reactions, using multiple heating rates. The theory is based on that $(\partial\alpha/\partial T) = k\mathrm{e}^{-E/RT} f(\alpha)$ and that the activation energy $E(\alpha)$ is constant for a certain conversion. The rate of the chemical reactions depends of the

Table 3
Adsorption parameters for the AlMCM-41 samples

Sample	S_{BET} ($m^2\,g^{-1}$)	V_t ($cm^3\,g^{-1}$)	a_o (nm)[a]	D_p (nm)	W_t (nm)[b]
AlMCM-41 (20)	803	0.47	4.18	2.32	1.86
AlMCM-41 (40)	894	0.58	4.16	2.59	1.57
AlMCM-41 (60)	658	0.38	4.23	2.12	2.11
AlMCM-41 (80)	525	0.35	4.39	2.72	1.67

[a] $a_o = 2d_{(100)}/\sqrt{3}$.
[b] $W_t = a_o - D_p$.

Table 4
Vibrational bands and its respective attributions observed in the uncalcined AlMCM-41 samples

Vibration bands (cm^{-1})	Attribution
3750–3250	Hydroxyl groups on mesoporous structure
3000–2850	Stretching of C—H bonds of CH_2 and CH_3 groups on CTMA+ species
1700–1550	Water physically adsorbed
1466–1460	Asymmetric deformation of CH_3—R bond
1475–1470	Deformation of CH_2 bond
1490–1480	Asymmetric deformation of head group methyl (CH_3—N+)
1260–1240	Asymmetric Si—O stretching
965–955	Asymmetric CH_3—N+ stretching
850–800	Symmetric T—O (T = Si, Al) stretching

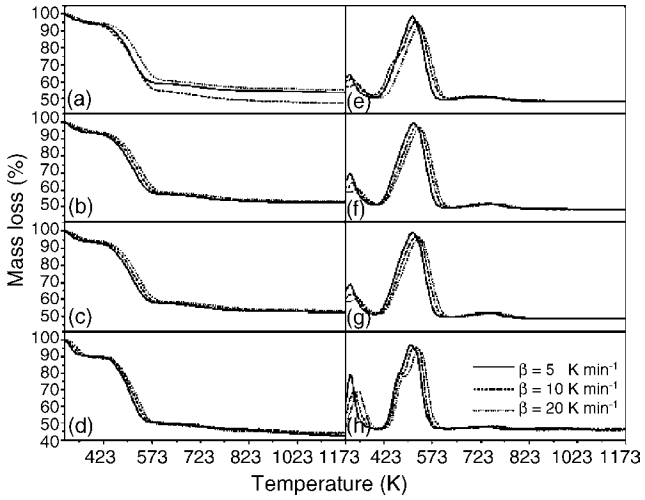

Fig. 3. TG curves of uncalcined AlMCM-41 at different heating rates: (a) Si/Al = 20; (b) Si/Al = 40; (c) Si/Al = 60; (d) SiAl = 80 and respective DTG curves; (e) and Si/Al = 20; (f) Si/Al = 40; (g) Si/Al = 60; (h) Si/Al = 80.

conversion (α), temperature (T) and time (t). The analysis is based on the isoconversion principle, which states that a constant conversion the reaction rate is only a function of the temperature. The basic equation of non-isothermal kinetics is as fallows:

$$\frac{d\alpha}{dT} = \frac{k}{\beta} f(\alpha) \tag{1}$$

where k is the rate constant (s^{-1}) and β the heating rate ($K\,s^{-1}$). Replacing k with the Arrhenius equation: $k = k_o e^{-E/RT}$ and rearranging gives:

$$\frac{1}{f_\alpha} d\alpha = \frac{k_\beta}{\beta} e^{-E/RT}\, dT \tag{2}$$

Integrating Eq. (2), gives:

$$\int_o^\alpha \frac{1}{f_\alpha} d\alpha = g(\alpha) = \frac{k_\beta}{\beta} \int_{T_o}^{T} e^{-E/RT}\, dT \tag{3}$$

Since $E/2RT \gg 1$, the temperature integral can be approximated by:

$$\int_{T_o}^{T} e^{-E/RT}\, dT \approx \frac{R}{E} T^2 e^{-E/RT} \tag{4}$$

Substituting the temperature integral, rearranging and logarithming, gives:

$$\ln \frac{\beta}{T_{\alpha,\beta^2}} = \ln \left[\frac{R k_o}{E_\alpha g(\alpha)} \right] - \frac{E_\alpha}{R} \frac{1}{T_{\alpha,\beta}} \tag{5}$$

In the typical experiment is necessary to obtain least at three different heating rates (β) and the respective conversion curves are evaluated from the measured TG curves. For each conversion (α), $\ln(\beta/T_{\alpha,\beta}{}^2)$ plotted versus $1/T_{\alpha,\beta}$, giving a straight line with slope $-E_\alpha/R$, therefore, the activation energy is obtained as function of the conversion. One of the greatest advantages of

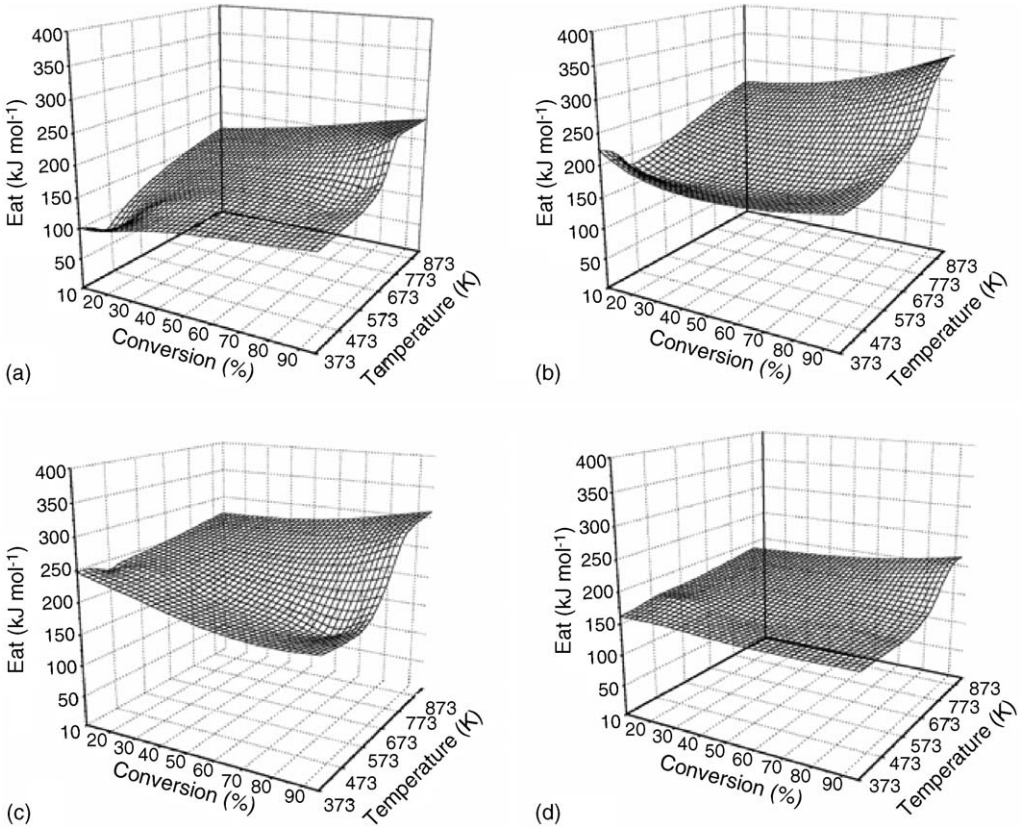

Fig. 4. Apparent activation energies to CTMA+ removal from AlMCM-41 materials varying the silicon/aluminium ratios, where (a) Si/Al = 20; (b) Si/Al = 40; (c) Si/Al = 60; (d) Si/Al = 80.

this model is the possibility to isolate the function $g(\alpha)$ in the linear coefficient. This function, mainly in complex process is very difficult to determine.

The kinetic data were obtained starting from TG measurements. Fig. 3 shows TG curves at different heating rates of AlMCM-41 samples with different Si/Al ratios in the uncalcined form and its respective DTG curves. We can observe three typical mass losses [11]: (i) from 303 to 373 K due to thermodesorption of physically adsorbed water; (ii) of 373 to 583 K due to the primary surfactant decomposition; (iii) 583 to 873 K due to residual surfactant decomposition and condensation of adjacent silanol groups resulting siloxane bonds. Fig. 4 presents the curves of the activation energy as function of conversion and temperature to each decomposition stage of CTMA+ from AlMCM-41 pores. The CTMA+ removal of the AlMCM-41 material was evaluated by thermogravimetry, at heating rates of 5, 10 and 20 K min^{-1}.

Fig. 4 presents the surface responses curves that represent the values of the apparent activation energy as function of the conversion degree and temperature for the removal of CTMA+ species occluded in the pores of the AlMCM-41 materials varying the Si/Al ratios of 20, 40, 60 and 80. As we can observe obtained values were of apparent activation energy in the range of 120–230 kJ mol^{-1}. A general rule was observed that an increase in the silicon/aluminium ratio results a gradual increase in the apparent activation energy. As showed in Fig. 4, the highest, the lowest and average values of the activation energy obeyed the following order of $E_{Si/Al}$: $E_{60} > E_{40} > E_{20}$ except for the sample with Si/Al = 80 that presented values activation energy (E_{80}) between E_{20} and E_{40}. Fig. 5 shows two comparative statistical graphics of the variation of the apparent activation energy with the Si/Al ratio. In Fig. 5a, the data were obtained through conversion degree and in Fig. 5b, through temperature data. Doing a comparative analysis of the obtained values of activation energy and the DRX data presented in Fig. 1 with the values showed in Fig. 5 can be observed the occurrence of a direct correspondence of crystallinity degree with the respective variation in the apparent activation energies to remove the template CTMA+ molecules. In this case it can be observed that more crystalline samples present typically larger variations in the apparent activation energy as function of conversion and temperature. This fact can be associated by the occurrence of diffusion limitations of heat and mass transfer for removal of the CTMA+ occluded in the pores of the AlMCM-41 materials. Samples of highly ordered structure present well-defined hexagonal pore structures that make difficult the elimination of the CTMA+ species due to combined existence of diffusion effects of heat transfer and mass transfer for removal of the species CTMA+ of the pores of the AlMCM-41 materials. In this case the existence of limitations to the transfer of heat and mass turns the diffusion step as slow, and controlling stage of the process obtains a more significant variation of the apparent activation energy with the variation of the temperature and conversion.

Another aspect to be considered is the possible occurrence of simultaneous series of complex events of CTMA+ decomposition. These complex events could not be evidenced in the curves TG and DTG in the studied conditions. In this case the decon-

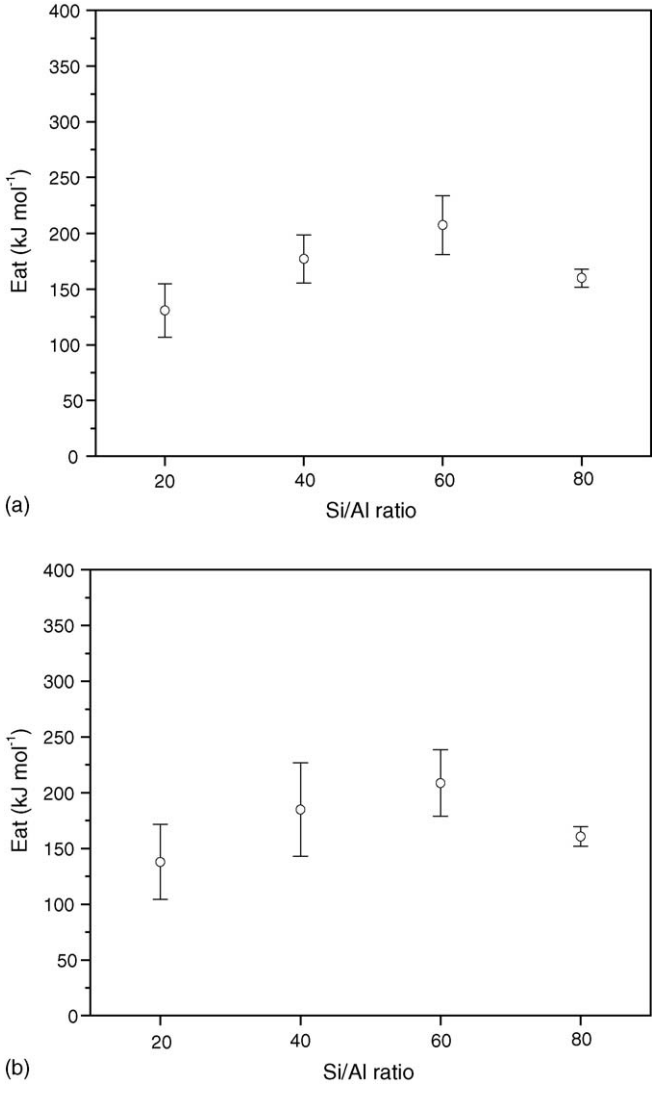

Fig. 5. Statistical distribution of the activation energy to removal of CTMA+ of the AlMCM-41 molecular sieve with different silicon/aluminium ratios, where (a) as functions of the conversion and (b) as function of the temperature.

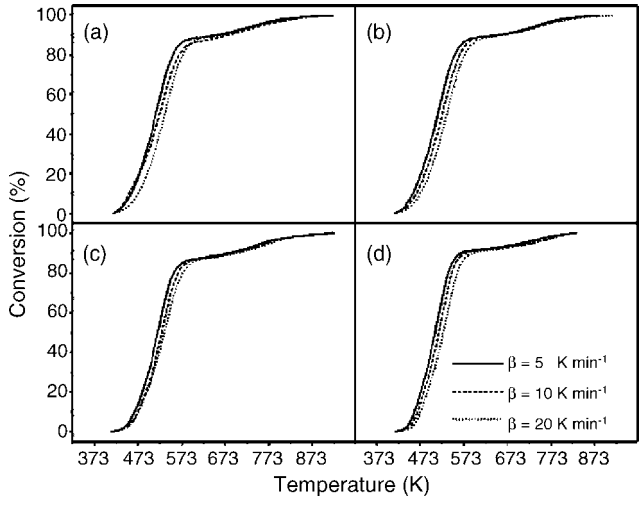

Fig. 6. Conversion curves of CTMA+ removal from AlMCM-41, where (a) Si/Al = 20; (b) Si/Al = 40; (c) Si/Al = 60; (d) Si/Al = 80.

volution was not possible. This also transforms it and analyzes isolated kinetics for each confused part, because the activation energy also varies a lot inside of each isolated event. In all cases observed two main events of mass loss were and these events can represent a series of complex reactions of CTMA+ decomposition (instead of simple events). In order to simplify the calculations only transformation stage was assumed. The obtained activation energy curves to each material were used coupled with the model-free algorithms [12–14] to estimation of conversion and isoconversion parameters at different stages of CTMA+ decomposition. Fig. 6 shows the conversion curves at three different heating rates as function of the temperature obtained by the model-free kinetics.

4. Conclusions

The present study shows that in non isothermal conditions, in which the uncalcined samples of AlMCM-41 with Si/Al ratios of 20, 40, 60 and 80 were heated at three different and constant heating rates, the model-free kinetic analysis shows a good alternative to estimate the apparent activation energy to remove the CTMA+ species. The apparent activation energies showed significant variations with the conversion degree and temperature and this variation have a relationship with the degree of crystallinity of the each sample that is proportional to the concentration of aluminium. Samples with more aluminium present high crystallinity degrees and consequently was observed at larger values of activation energy to the removal of CTMA+ of the pore system.

Acknowledgements

The authors wish to acknowledge the financial support provided by Rede Norte-Nordeste de Catálise (RECAT), Rede Petrogas de Sergipe and Conselho Nacional de Desenvolvimento Científico e Tecnológico (CNPq).

References

[1] X.S. Zhao, G.Q. Lu, G.J. Millar, Ind. Chem. Res. 35 (1996) 2075.
[2] J.S. Beck, J.C. Vartuli, W.J. Roth, M.E. Leonowicz, C.T. Kresge, K.D. Schmitt, C.T.W. Chu, D.H. Olson, E.W. Sheppard, S.B. McCullen, Y.B. Higgins, I.L. Schelenker, J. Am. Chem. Soc. 114 (1992) 10834.
[3] I.K. Mbaraka, B.H. Shanks, J. Catal. 229 (2005) 365.
[4] B.R. Jermy, A. Pandurangan, Appl. Catal. A: Gen. 288 (2005) 25.
[5] C.T. Kresge, M.E. Leonowicz, W.J. Roth, J.C. Vartuli, J.S. Beck, Nature 359 (1992).
[6] S.K. Badamali, A. Sakthivel, P. Selvam, Catal. Today 63 (2000) 291.
[7] M. Busio, J. Janchen, J.H.C. Van Hoff, Microporous Mesoporous Mater. 5 (1995) 211.
[8] Y. Cesteros, G.L. Haller, Microporous Mesoporous Mater. 43 (2001) 171.
[9] A.S. Araujo, M. Jaroniec, Thermochim. Acta 363 (2000) 175.
[10] S. Kawi, W. Lai, AIChE J. 48 (2002) 1572.
[11] S.A. Araujo, M. Ionashiro, V.J. Fernandes Jr., A.S. Araujo, J. Therm. Anal. Calorim. 64 (2001) 801.
[12] S. Vyazovkin, V. Goryachko, Thermochim. Acta 194 (1992) 221.
[13] S. Vyazovkin, Int. J. Chem. Kinet. 28 (1996) 95.
[14] S. Vyazovkin, C.A. Wright, Thermochim. Acta 340 (1999) 53.
[15] B. Marler, U. Oberhagemann, S. Vortmann, H. Gies, Microporous Mesoporous Mater. 6 (1996) 375.
[16] S.C. Shen, S. Kavi, J. Phys. Chem. B 103 (1999) 8870.
[17] A.S. Araujo, C.D.R. Souza, M.J.B. Souza, V.J. Fernandes Jr., L.A.M. Pontes, Stud. Surf. Sci. Catal. 141 (2002) 467.
[18] S. Brunauer, P.H. Emmett, E. Teller, J. Am. Chem. Soc. 60 (1938) 309.
[19] E.P. Barrett, L.J. Joyner, P.P. Halenda, J. Am. Chem. Soc. 73 (1951) 373.
[20] D.C. Calabro, E.W. Valyocsik, F.X. Ryan, Microporous Mesoporous Mater. 7 (1997) 243.